Available online at www.sciencedirect.com
ScienceDirect
Thin Solid Films 516 (2008) 2094–2098
www.elsevier.com/locate/tsf

Fabrication and magnetization measurement of Ni thin films on silicon substrate by electrodeposition

Yang Tang [a,b], Dongxu Zhao [a,*], Dezhen Shen [a], Jiying Zhang [a], Binghui Li [a], Youming Lu [a], Xiwu Fan [a]

[a] *Key Laboratory of Excited State Process, Changchun Institute of Optics, Fine Mechanics and Physics, Chinese Academy of Sciences, 16 East Nan-Hu Road, Open Economic Zone, Changchun 130033, People's Republic of China*
[b] *Graduate School of the Chinese Academy of Sciences, People's Republic of China*

Received 28 April 2007; received in revised form 19 November 2007; accepted 20 November 2007
Available online 31 December 2007

Abstract

Ni thin films were electrodeposited on n-Si (100) substrate from the electrolytes containing $Ni(CH_3COO)_2$ and CH_3COONH_4 at room temperature. The scanning electron microscope images of the films reveals the uniform distribution of the nickel all over the substrate surface, which illustrates that the fine Ni films on large scales could be obtained through the method of electrodeposition. Vibrating sample magnetometer measurement with the applied field parallel to the surface shows obvious hysteresis loops of the magnetic thin films. The morphology and magnetism of the Ni thin films evolves with the deposition time increasing. The effect of deposition conditions on the properties of the Ni thin films is investigated.

Keywords: Electrochemistry; Deposition process; Nickel; Magnetic properties; Measurements

1. Introduction

The integration of ferromagnetic films with semiconductors is essential for the realization of a number of prospective devices based on spin-dependent transport, such as spin field effect transistors and spin light emitting diodes [1]. Electrodeposition presents some advantages for fabricating ferromagnetic thin films on semiconductors, such as low temperature processing, low cost owing to the unnecessary of either high vacuum or high temperature and high deposition rates. It was reported that the Ni thin films had been electrodeposited on GaAs, which showed interfaces exhibited limited or no intermixing [2]. Electrodeposition is an excellent method for the production of epitaxial and sharp interfaces, since the process occurs at low temperature, and the incoming atoms are consequently deposited at very low energies, limiting interdiffusion during deposition [3].

In this work electrodeposition is used to prepare Ni thin films on n-type Si substrates. The semiconducting substrates are used

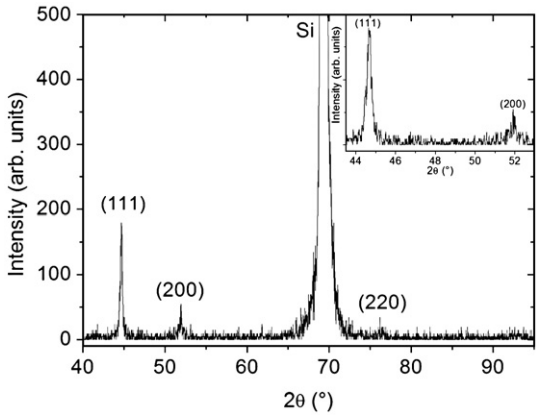

Fig. 1. XRD patterns of Ni thin films deposited on silicon from 0.01 M Ni $(CH_3COO)_2$ and 0.05 M CH_3COONH_4 electrolytes for 30 min. Inset: the enlarged view of the peaks (111) (200) of nickel thin films.

* Corresponding author. Tel.: +86 431 86176322; fax: +86 431 84627031.
E-mail address: dxzhao2000@yahoo.com.cn (D. Zhao).

0040-6090/$ - see front matter © 2007 Elsevier B.V. All rights reserved.
doi:10.1016/j.tsf.2007.11.095

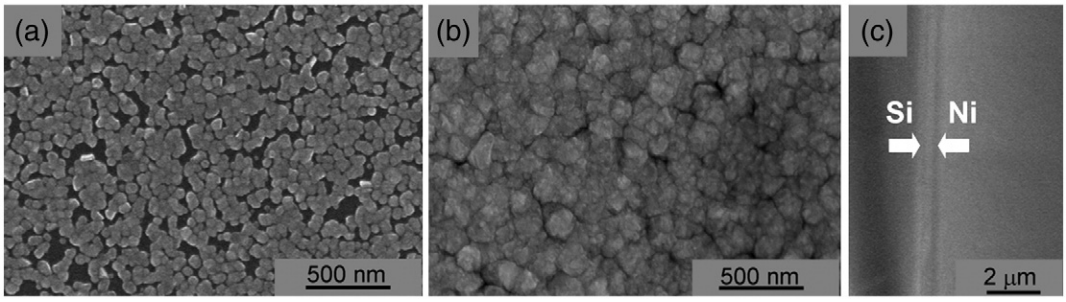

Fig. 2. SEM images of Ni thin films deposited on silicon from 0.01 M $Ni(CH_3COO)_2$ and 0.05 M CH_3COONH_4 electrolytes for (a) 1 min (b) 10 min (c) cross section (the area indexed by the arrows) of Ni thin films deposited for 30 min. The scale bar is 500 nm for (a) (b) and is 2 μm for (c). The SEM operating voltage was 15 kV for (a) (b) and 18 kV for (c).

to integrate a convenient method for fabricating thin magnetic films with silicon technology [4]. The research in this paper developed a composing of the electrolytes for producing high quality nickel deposits, which have the advantage of being environmentally friendly.

2. Experimental section

n-Si (100) wafers were used as substrates. After standard chemical cleaning and a dip in 5% HF solution, the wafers were rinsed with deionized water and then immediately transferred to the electrodeposition cell with a Pt counter electrode and an Ag/AgCl reference electrode. The Ni thin films on Si were prepared from aqueous electrolytes containing $Ni(CH_3COO)_2$ as the source of metal ions, and CH_3COONH_4 as supporting electrolyte.

X-ray diffraction (XRD) patterns of the films were taken on a Siemens D500 diffractometer operating in the θ–2θ Bragg configuration using CuK_a radiation of 1.5418 Å. The surface morphology of the films was observed with a scanning electron microscope (SEM). The SEM operating voltage was 15 kV for Fig. 2(a) and (b), 18 kV for (c) and 10 kV for Fig. 5(a)–(d). Magnetic characteristics were studied using a vibrating sample magnetometer (VSM) (Lake Shore Company) at room temperature.

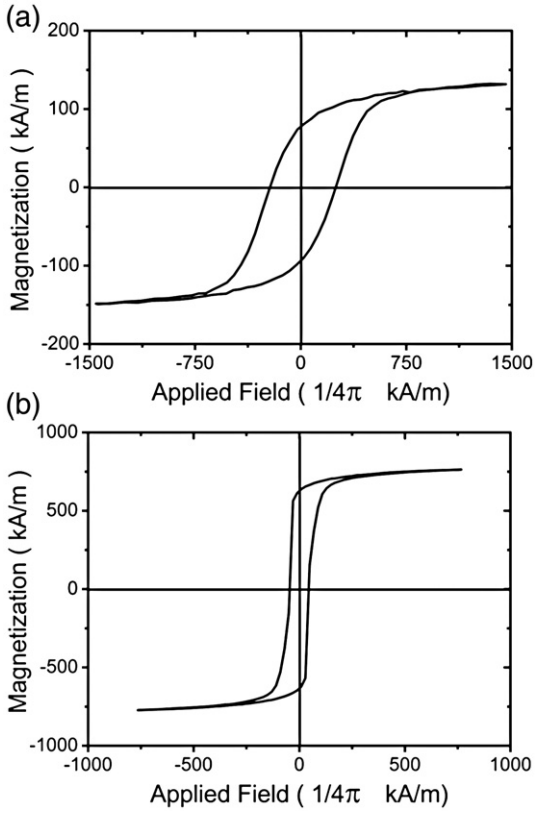

Fig. 3. VSM hysteresis loop for Ni thin films deposited from 0.01 M Ni $(CH_3COO)_2$ and 0.05 M CH_3COONH_4 electrolytes for (a) 1 min (b) 10 min. The magnetic field was applied parallel to the film surface.

3. Results and discussion

The Ni films deposition strongly depends on the experimental parameters of electrodeposition. The Ni thin films with the silver metallic luster could be deposited from the electrolytes containing $Ni(CH_3COO)_2$ and CH_3COONH_4. However, it is impossible to deposit the Ni films from the electrolytes without CH_3COONH_4 under the same experimental conditions. Even when we changed growth parameters, such as the applied potentials, the growth time, the bath temperature and the concentration of the electrolytes, Ni films could not be obtained without the addition of CH_3COONH_4. This result indicates that CH_3COONH_4 plays a very important role during the deposition of the Ni thin films. Moreover, when the concentration of CH_3COONH_4 was lower than 0.05 M, no Ni film was obtained on Si substrate. The effect of deposition conditions on the properties of the Ni thin films is explored. But

Table 1
The deposition conditions of Ni thin films for sample A, B, C, D

	Electrolyte		Applied potential (V)	Temperature (°C)	Growth time (min)
Sample A	$Ni(CH_3COO)_2$	0.05 M	−1.15	RT	10
	CH_3COONH_4	0.05 M			
Sample B	$Ni(CH_3COO)_2$	0.05 M	−1.20	RT	10
	CH_3COONH_4	0.05 M			
Sample C	$Ni(CH_3COO)_2$	0.05 M	−1.15	45	10
	CH_3COONH_4	0.05 M			
Sample D	$Ni(CH_3COO)_2$	0.1 M	−1.15	RT	10
	CH_3COONH_4	0.05 M			

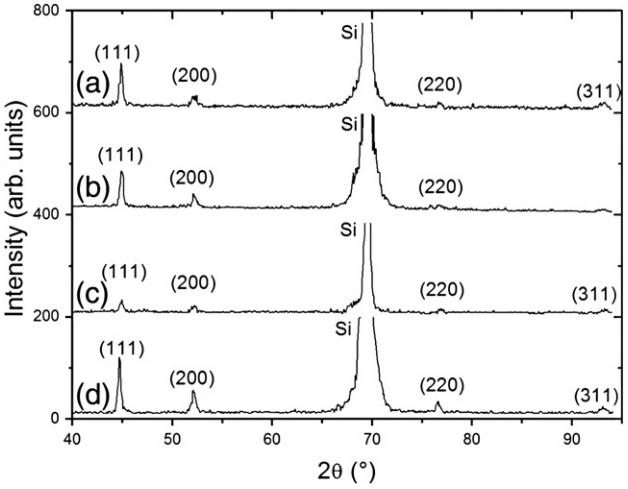

Fig. 4. XRD patterns of Ni thin films for sample A, B, C, D.

at higher growth temperature the diffusion of Ni atoms into the silicon substrate may be promoted [5].

Fig. 1 shows the XRD pattern of the films electrodeposited for 30 min from 0.01 M $Ni(CH_3COO)_2$. As can be seen in Fig. 1, the diffraction peaks located at 44.6°, 51.9° and 76.2° correspond to (111) (200) and (220) directions of face-centred cubic structure Ni. No diffractive peaks of other impurities are detected in this pattern.

Fig. 2(a) shows the morphology of the sample after deposition for 1 min. The Ni film is composed of the small crystalline nanoparticles with diameters ranging from 50 to 100 nm. And the substrate could not be entirely covered by these nanoparticles. It is certain that the nucleation of crystalline nanoparticles began from some sites on the silicon substrate and the nanoparticles became connected to each other with continuous growing of the crystallites. When the time of the deposition increased to 10 min, as illustrated in Fig. 2(b), the surface of the silicon slice is entirely covered by the compact Ni film. The Ni films are composed of compactly stacked Ni crystallites. The SEM images of the films reveal the uniform distribution of the nickel all over the surface of the substrate. Fig. 2(c) shows the cross section of Ni thin films deposited for 30 min. It can be observed that the thin films on the substrate are uniform in large area with approximate thickness of 500 nm.

VSM measurements were performed on the Ni films electrodeposited from electrolytes containing 0.01 M Ni $(CH_3COO)_2$ and 0.05 M CH_3COONH_4. Fig. 3(a) and (b) show the hysteresis loops recorded with the applied field parallel to the surfaces of the samples deposited for 1 min and 10 min, respectively. It is clear that coercivity depends strongly on the film thickness. For the sample grown for 1 min the coercivity and the saturation magnetization are 131 kA m^{-1} and 77 kA m^{-1}, respectively. The saturation magnetization is smaller than that of the bulk materials (484 kA m^{-1}) [6]. But when increasing the growth time to 10 min, the saturation magnetization is 761 kA m^{-1}, which is larger than that of the bulk materials. The coercivity is as low as 3.5 kA m^{-1}, which is 5 times smaller than the sample deposited for 1 min. This result suggests that the coercivity decreases with the increase of the film thickness, which is due to the enhancement of magnetic dipole interactions that results in decreasing the coercive force. The decrease in coercivity with increasing thickness is consistent with Néel's theoretical predictions for the domain wall motion coercivity mechanism [7]. Calculation of the thickness dependence of the coercivity is performed by general expression as $Hc=At^{-n}$ where t is film thickness and A,n are fitting constant [8].

In order to investigate the effect of deposition conditions on the properties of the Ni thin films, four samples under different growth parameters were fabricated. Table 1 shows the deposition conditions for these samples that are marked with A, B, C and D. Fig. 4 shows the XRD patterns of these samples. As can be seen in Fig. 4(a), the XRD diffraction peaks located at 44.9°, 52.2°, 76.6° and 93.3° corresponding to (111), (200)

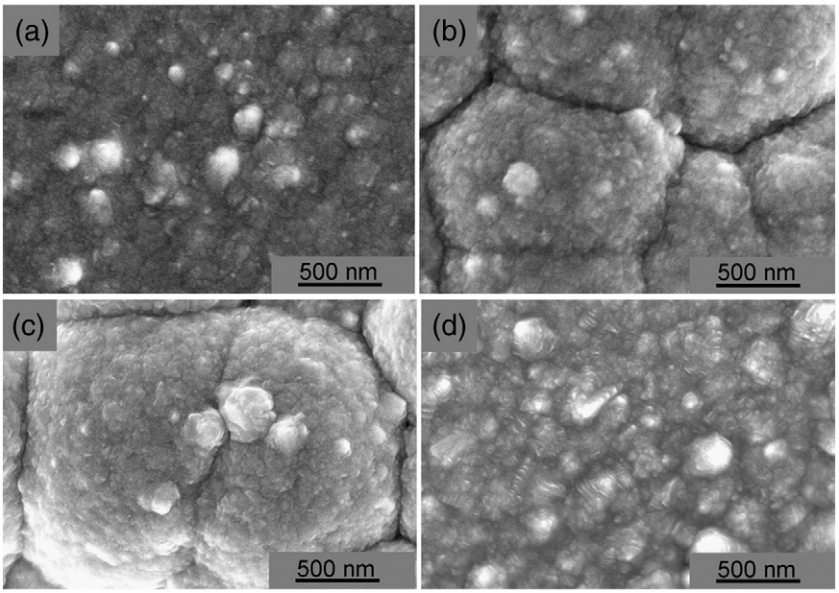

Fig. 5. SEM images of Ni thin films for (a)sample A (b)sample B (c) sample C (d) sample D. The SEM operating voltage was 10 kV.

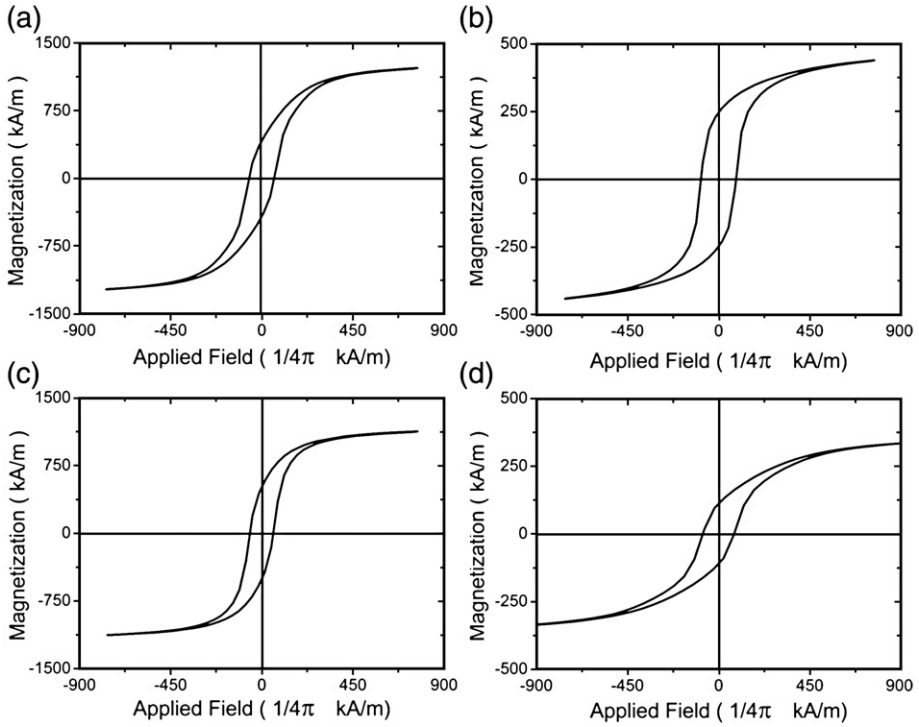

Fig. 6. VSM hysteresis loop for Ni thin films for (a)sample A (b)sample B (c) sample C (d) sample D. The magnetic field was applied parallel to the film surface.

(220) and (311) directions of face-centred cubic structure Ni. As the applied potential was increased to −1.2 V, the peak at (311) orientation almost disappeared. Fig. 4(c) shows that the intensities of Ni peaks decrease when the growth temperature was increased to 45 °C. As $Ni(CH_3COO)_2$ was increased to 0.1 M, the intensities of Ni peaks increased. No diffractive peaks of other impurities are detected in all these XRD patterns. The mean grain sizes of the films are evaluated by using the Debye–Scherer formula [9]:

$$D = 0.9\lambda/B\cos\theta_B$$

Where λ is the X-ray wavelength (1.5418 Å), θ_B is the Bragg diffraction angle, and B is the FWHM (full widths at half-maximum). The mean grain sizes of the samples for A, B, C and D are 26.9, 26.1, 22.2 and 30.9 nm, respectively.

Fig. 5 shows the morphology of the sample A, B, C and D. As can be seen in Fig. 5(a), The Ni films electrodeposited from 0.05 M $Ni(CH_3COO)_2$ and 0.05 M CH_3COONH_4 at −1.15 V for 10 min at room temperature are composed of compactly stacked Ni crystallites. The surface of the silicon slice is entirely covered by the compact Ni film. As the applied potential was increased to −1.2 V, the Ni films are composed of Ni clusters with obvious boundaries indicated in Fig. 5(b). The Ni films of sample C which was at the growth temperature of 45 °C shows similar morphology. As $Ni(CH_3COO)_2$ was increased to 0.1 M, the Ni films are also composed of stacked Ni crystallites.

VSM measurements were performed on the Ni films of sample A B C D. Fig. 6 shows the hysteresis loops recorded with the applied field parallel to the surfaces of the samples. As can be seen in Fig. 6(a), the coercivity and saturation magnetization of the Ni films (sample A) are 5.0 kA m^{-1} and 1225 kA m^{-1}, respectively. As the applied potential was increased to −1.2 V, the coercivity and the saturation magnetization of the Ni films (sample B) are 7.0 kA m^{-1} and 437 kA m^{-1}. The coercivity and the saturation magnetization of sample C which was at the growth temperature of 45 °C are 4.6 kA m^{-1} and 1229 kA m^{-1}. The saturation magnetizations of sample A and C are larger than those of the bulk materials (484 kA m^{-1}). As $Ni(CH_3COO)_2$ was increased to 0.1 M, the coercivity and the saturation magnetization of the Ni films (sample D) are 6.2 kA m^{-1} and 332 kA m^{-1}. The saturation magnetizations of sample B and D are smaller than those of the bulk materials.

4. Conclusion

In summary, we have deposited fine Ni films on n-Si with silver metallic luster from the electrolytes containing $Ni(CH_3COO)_2$ and CH_3COONH_4. The morphology of Ni thin films evolves with increasing the deposition time. And the coercivity decreases with the increase of the film thickness while the magnetic field was applied parallel to the film surface, which is attributed to the magnetic dipole interaction. The decrease in coercivity with increasing thickness is consistent with Néel's theoretical predictions for the domain wall motion coercivity mechanism. The Ni thin films fabricated under different deposition conditions show different structural, morphological and magnetic properties.

Acknowledgement

This work is supported by the Key Project of National Natural Science Foundation of China under Grant No. 60336020, No.

50532050, the "973" program under Grant No. 2006CB604906, the CAS Innovation Program, the National Natural Science Foundation of China under Grant No. 60429403, No. 60506014, No. 50402016 and No. 10674133.

References

[1] S.A. Wolf, D.D. Awschalom, R.A. Buhrman, J.M. Daughton, S. von Molnar, M.L. Roukes, A.Y. Chtchelkanova, T.M. Treger, Science 294 (2001) 1488.
[2] C. Scheck, P. Evans, G. Zangari, R. Schad, Appl. Phys. Lett. 82 (2003) 2853.
[3] G. Bubbiotti, G. Carlotti, S. Tacchi, Y.K. Liu, C. Scheck, R. Schad, G. Zangari, J. Appl. Phys. 97 (2005) 10J102.
[4] M.L. Munford, L. Seligman, M.L. Satrorelli, E. Voltoline, L.F.O. Martins, W. Schwarzacher, A.A. Pasa, J. Magn. Magn. Mater. 226–230 (2001) 1613.
[5] Y.J. Chang, J.L. Erskine, Phys. Rev., B 28 (1983) 5766.
[6] G.M. Chow, J. Zhang, Y.Y. Li, J. Ding, W.C. Goh, Mater. Sci. Eng., A 304–306 (2001) 194.
[7] Q. Zeng, I. Baker, Y. Sun, J.B. Cui, C.P. Daghlian, J. Appl. Phys. 99 (2006) 08M302.
[8] J.G. Kim, K.H. Han, S.H. Song, A. Reilly, Thin Solid Films 440 (2003) 54.
[9] B.D. Cullity, Elements of X-ray Diffractions, Addition-Wesley, Reading, MA, 1978, p. 102.